

Carpet-2 search for gamma rays above 100 TeV in coincidence with HAWC and IceCube alerts

D. D. Dzheppuev^a, Yu. Z. Afashokov^a, I. M. Dzaparova^{a,b}, E. A. Gorbacheva^a, I. S. Karpikov^a, M. M. Khadzhiev^a, N. F. Klimenko^a, A. U. Kudzhaev^a, A. N. Kurenova^a, A. S. Lidvansky^a, O. I. Mikhailova^a, V. B. Petkov^{a,b}, V. S. Romanenko^a, G. I. Rubtsov^a, S. V. Troitsky^{a1}, I. B. Unatlov^a, A. F. Yanin^a, Ya. V. Zhezher^a, K. V. Zhuravleva^a

^a*Institute for Nuclear Research of the Russian Academy of Sciences,
60th October Anniversary prospect 7A, 117312 Moscow, Russia*

^b*Institute of Astronomy, Russian Academy of Sciences, Moscow, 119017 Russia*

Submitted November 4, 2020

We report on the search of astrophysical gamma rays with energies in the 100 TeV to several PeV range arriving in directional and temporal coincidence with public alerts from HAWC (TeV gamma rays) and IceCube (neutrinos above ~ 100 TeV). The observations have been performed with the *Carpet-2* air-shower detector at the Baksan Neutrino Observatory, working in the “photon-friendly” mode since 2018. Photon candidate showers are selected by their low muon content. No significant excess of the photon candidates have been observed, and upper limits on gamma-ray fluences associated with the alerts are obtained. For events with good viewing conditions, the *Carpet-2* effective area for photons is of the order of the IceCube effective area for neutrinos of the same energy, so the constraints start to probe the production of neutrinos in fast flares of Galactic sources.

Over the last decade, multimessenger astronomy has brought several bright results of great importance, notably the identification of a binary neutron star merger in gravitational-wave and electromagnetic channels [1] and a possible association of a high-energy neutrino event with a blazar flare [2]. These and other important observations became possible thanks to alerts distributed by gravitational-wave, neutrino and conventional astronomical observatories to the worldwide community of observers detecting signals in various channels and electromagnetic bands. Up to now, in the electromagnetic channel, these alerts have been followed up at the energies up to ~ 100 TeV, above which the sensitivity of the highest-energy participating observatory, HAWC, fades, while higher energies have been accessible only for the neutrino and cosmic-ray channels. The purpose of the present paper is to push further this high-energy limit for the photon channel and to report the results of the first ever multimessenger alert follow-up in the 100 TeV to several PeV gamma-ray band.

This energy band is especially important for high-energy neutrino alerts because it is precisely the range where the estimated neutrino energies fall to. The origin of these astrophysical neutrinos remains uncertain, see e.g. Refs. [3, 4] for reviews. Recent studies indicate [5, 6] that the entire astrophysical neutrino flux between 1 TeV and 1 PeV, estimated from muon-track events

and extrapolated to lower energies as a power law [7], may be associated with radio blazars. However, analyses of cascade events [8] indicate that this extrapolation may underestimate the flux at several tens TeV. The origin of the additional flux component is unknown, and some Galactic scenarios are discussed [9]. Note that these putative Galactic sources may be distributed isotropically in the sky because of constraints on the excess of neutrino emission from the Galactic plane [10, 11].

In the dominant part of the scenarios of the astrophysical production of high-energy neutrinos, they are born in π^\pm -meson decays, while the decays of π^0 mesons result in the accompanying gamma rays of similar energies. The $\sim (100 \dots 1000)$ TeV photons efficiently produce e^\pm pairs on the cosmic microwave background [12], so the mean free path of these photons does not exceed the size of the Milky Way. Therefore, photons of these energies cannot reach us from active galactic nuclei (see e.g. Ref. [13] for a discussion of models), nor from putative neutrino production regions in the intergalactic space [14, 15]. Any observation of gamma rays at these energies associated with neutrinos would either imply Galactic sources [16, 17] or, if the event is directionally associated with an extragalactic object, suggest new particle physics affecting the transparency of the Universe to high-energy gamma rays [18].

¹Corresponding author; e-mail: st@ms2.inr.ac.ru

Previously, we reported [19] on the analysis of the data above 1 PeV accumulated by Carpet-2 during 1999–2011, when the main task of the experiment was related to cosmic-ray studies. We obtained constraints on the neutrino flux from directions of IceCube neutrinos assuming the sources are steady, because the data time spans did not overlap. Since 2018, Carpet-2 returned to data taking, now as a gamma-ray observatory: changes in the trigger and in the data analysis allowed us to significantly improve the efficiency and to lower the threshold energy for gamma-ray studies, see e.g. Ref. [20]. Here, we report for the first time on the results of simultaneous observations of the alerts at energies above 100 TeV.

IceCube issues public alerts corresponding to detections of individual muon-track events passing certain criteria since 2017, see the description of “EHE” and “HESE” alerts (2017–2019) in Ref. [21] and of “GOLD” and “BRONZE” alerts (since 2019) in Ref. [22]. Most of the alert events have estimated energies between 100 TeV and 1 PeV. The criteria are chosen to maximize the probability that the event is of astrophysical origin. Still, many of them are background atmospheric events: the astrophysical purity of the “GOLD” sample is only 50%, that of the “BRONZE” sample is 30%.

Another window into sub-PeV astrophysics is provided by observations of gamma rays at slightly lower energies in the TeV range. In parallel with pointing observations by atmospheric Cerenkov telescopes, air-shower installations monitor the sky continuously. In particular, HAWC has recently started to issue various public alerts when a significant point-like signal is observed during one daily passage of the “flare” direction through the HAWC field of view, see Ref. [23] for more details. These alerts are of particular interest because the energies are very close to the band we study here, and a discovery of a flaring Galactic source in this energy range would have important astrophysical consequences.

We report here on the results of 2.5 years of following up these HAWC and IceCube alerts with Carpet-2, see Refs. [24, 25] for the description of the experiment. Since Carpet-2 is an air-shower detector, it operates continuously and observes a large fraction of the sky. Therefore it does not need to be pointed to the alert direction, so the alerts are analysed offline. The search is based on the set of photon candidate events which are selected as muon-poor air showers, as described in Refs. [19, 20, 26]. The photon detection efficiency and the angular resolution were determined by the Monte-Carlo simulations; together with the photon-candidate

Energy, TeV	Min. N_e	Max. n_μ/N_e	Selection efficiency	Number of events
>100	$10^{4.2251}$	0	0.995	1021
>300	$10^{4.6372}$	0	0.509	598

Table 1: Two samples of photon candidate events.

selection cuts for the energies $E > 300$ TeV they are discussed in detail in Ref. [20] (“Dataset II”). Here, we extend the analysis down to 100 TeV energies because the combined directional and temporal selection reduces efficiently the hadronic background, which otherwise is the main problem in the search for gamma rays with Carpet-2 below 300 TeV. Photon candidate events are selected by their reconstructed number of charged particles, N_e , and the number of muons in the 175 m² muon detector, n_μ . It was found optimal to consider only muonless events for these energies, though at higher energies the cut was determined in terms of the ratio n_μ/N_e . The criteria are given in Table 1 together with the number of photon candidate events in the data sample and the efficiency of the gamma-ray selection cuts (determined as the ratio of Monte-Carlo photons with reconstructed n_μ , N_e satisfying the selection conditions to the total number of reconstructed Monte-Carlo photons). The candidates were selected from 52791 air showers, recorded between April 8, 2018, and October 26, 2020, successfully reconstructed and passing the quality cuts. The number of live days in this period was 675.

Carpet-2 dataset consists of events being observed with zenith angles up to 40°, but the efficiency decreases fastly for inclined showers. We select the alerts with declinations between +5° and +76° so that the maximal elevation corresponds to a zenith angle not exceeding 35°. In addition, we drop the events arrived at the days when our data were not recorded because of maintenance. In this way we arrive to the list of 9 HAWC alerts and 22 IceCube alerts presented in Table 2 in the Supplementary Material [27].

Most of the alert directions, however, were outside the Carpet-2 field of view at the moment of the event, but they passed through the field of view during the day. We therefore determine time windows of 24 hours and of 30 days, centered at the event moment, to search for coinciding gamma-ray candidates. The angular window, as discussed before [20], was set to the 90% CL angular resolution, which at these energies is about 6.15°. The expected number of candidate events was calculated by

randomizing arrival times of photon candidates in the sample.

For each particular alert we present the expected and observed numbers of the events, the estimated flux within the selected time window and the fluence in Tables 3, 4 in the Supplementary Material [27]. Note that the flux estimates depend crucially on the time window, which is chosen more or less arbitrarily, while the most interesting physical quantity for a burst is the fluence. No significant excess of photon candidates was found, and we present 95% CL upper limits on the flux and fluence. These limits vary strongly from one alert to another because of the strong dependence of the reconstruction efficiency for photons on the zenith angle. In all cases we are close to the “zero signal, zero background” regime which motivates us to use stacking to improve sensitivity, and stacked results for all HAWC alerts and all IceCube alerts are also presented in the same tables.

A weak, two-sigma excess, 8 events observed for 4.25 expected, is found at $E > 100$ TeV for stacked IceCube events, dominated by the 200911A alert. This excess is consistent with expected fluctuations, given multiple trials.

Directions of two IceCube events, 190331A and 191215A, were in the Carpet-2 field of view at the moment of neutrino arrivals, which allows us to estimate directly their fluence assuming a fast flare. We use the time window of 1000 s for these two alerts. For good viewing conditions, that is small zenith angles, the effective area of Carpet-2 in the configuration used for the photon search in the present analysis is of the same order as the effective area of IceCube for neutrinos of similar energies, see Fig. 1. Therefore, the fluence upper limits of order $\lesssim 1$ GeV/cm², see Tables 3, 4, 5 in the Supplemental material [27], start to constrain the origin of neutrinos in fast flares of Galactic sources. Assuming flares longer than a few hours, we obtain less constraining limits because the arrival direction of the alert event leaves the field of view of Carpet-2. All HAWC alerts happen outside of the Carpet-2 field of view because of the difference in geographical longitudes of the two installations.

The program of multimessenger observations with Carpet-2 continues. Besides HAWC and IceCube alerts, it includes also LIGO/VIRGO alerts and low-energy neutrino burst alerts from the Baksan Underground Scintillator Telescope. Soon, when Baikal-GVD high-energy neutrino alerts become available, they will join the list. At the same time, the upgrade of the installation to Carpet-3 is ongoing with an order of magnitude increase in the collection area and more than a twofold

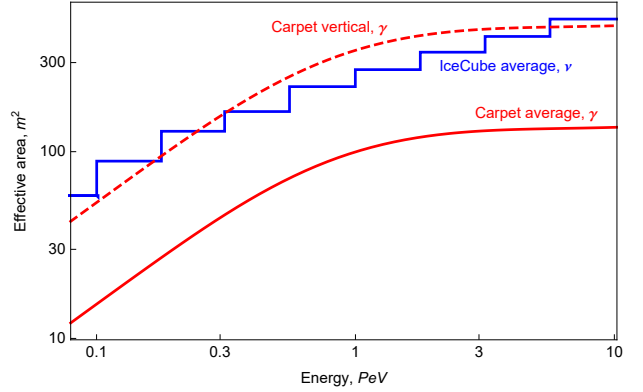


Figure 1: Comparison of effective areas of Carpet-2 (red continuous lines, photon detection, present analysis) and IceCube (blue step line, neutrino detection, muon tracks, average over the Northern hemisphere [28]). For Carpet-2, the full line gives the average over the field of view while the dashed line corresponds to vertical events.

increase in the area of the muon detector. This will allow to reach the sensitivity in the sub-PeV gamma rays at the level of the corresponding neutrino sensitivity of IceCube not only for short flares, but also for long-term observations and for the diffuse flux.

This work is supported in the framework of the State project “Science” by the Ministry of Science and Higher Education of the Russian Federation under the contract 075-15-2020-778.

1. B. P. Abbott, R. Abbott, T. D. Abbott *et al.* *Astrophys. J. Lett.* **848** (2017) L12 [arXiv:1710.05833 [astro-ph.HE]].
2. M. G. Aartsen *et al.*, *Science* **361** (2018) no.6398, eaat1378 [arXiv:1807.08816 [astro-ph.HE]].
3. M. Ahlers and F. Halzen, *Prog. Part. Nucl. Phys.* **102** (2018) 73 [arXiv:1805.11112 [astro-ph.HE]].
4. A. Palladino, M. Spurio and F. Vissani, *Universe* **6** (2020) 30 [arXiv:2009.01919 [astro-ph.HE]].
5. A. Plavin, Y. Y. Kovalev, Y. A. Kovalev and S. Troitsky, *Astrophys. J.* **894** (2020) 101 [arXiv:2001.00930 [astro-ph.HE]].
6. A. V. Plavin, Y. Y. Kovalev, Y. A. Kovalev and S. V. Troitsky, arXiv:2009.08914 [astro-ph.HE].
7. J. Stettner [IceCube], *PoS ICRC2019* (2020), 1017 [arXiv:1908.09551 [astro-ph.HE]].
8. M. G. Aartsen *et al.* [IceCube], *Phys. Rev. Lett.* **125** (2020) 121104 [arXiv:2001.09520 [astro-ph.HE]].
9. A. Palladino and F. Vissani, *Astrophys. J.* **826** (2016) 185 [arXiv:1601.06678 [astro-ph.HE]].
10. S. Troitsky, *JETP Lett.* **102** (2015) no.12, 785 [*Pisma Zh. Eksp. Teor. Fiz.* **102** (2015) no.12, 899] [arXiv:1511.01708 [astro-ph.HE]].

11. A. Albert *et al.* [ANTARES and IceCube], *Astrophys. J. Lett.* **868** (2018) no.2, L20 doi:10.3847/2041-8213/aaecef [arXiv:1808.03531 [astro-ph.HE]].
12. A.I. Nikishov, *Sov. Phys. JETP* **14** (1962) 393 [*ZhETF* **41** (1962) 549].
13. M. Cerruti, *J. Phys. Conf. Ser.* **1468** (2020) 012094 [arXiv:1912.03666 [astro-ph.HE]].
14. M. Kachelrieß, O. Kalashev, S. Ostapchenko and D. V. Semikoz, *Phys. Rev. D* **96** (2017) 083006 [arXiv:1704.06893 [astro-ph.HE]].
15. A. V. Uryson, *Phys. Rev. D* **100** (2019) 083019 [arXiv:1906.01014 [astro-ph.HE]].
16. M. Ahlers and K. Murase, *Phys. Rev. D* **90** (2014) 023010 [arXiv:1309.4077 [astro-ph.HE]].
17. O. E. Kalashev and S. V. Troitsky, *JETP Lett.* **100** (2015) 761 [*Pisma Zh. Eksp. Teor. Fiz.* **100** (2014) 865] [arXiv:1410.2600 [astro-ph.HE]].
18. S. V. Troitsky, *JETP Lett.* **105** (2017) 55 [arXiv:1612.01864 [astro-ph.HE]].
19. D. D. Dzhappuev, I. M. Dzaparova, E. A. Gorbacheva *et al.* *JETP Lett.* **109** (2019) 226 [arXiv:1812.02662 [astro-ph.HE]].
20. D. D. Dzhappuev, I. M. Dzaparova, E. A. Gorbacheva *et al.* *PoS ICRC2019* (2020), 808 [arXiv:1907.10893 [astro-ph.HE]].
21. M. G. Aartsen *et al.* [IceCube], *Astropart. Phys.* **92** (2017) 30 [arXiv:1612.06028 [astro-ph.HE]].
22. E. Blaufuss *et al.* [IceCube], *PoS ICRC2019* (2020), 1021 [arXiv:1908.04884 [astro-ph.HE]].
23. J. R. Wood, Ph.D. Dissertation, Department of Physics, University of Maryland, [arXiv:1801.01550 [astro-ph.HE]].
24. J. Szabelski [Carpet-3 Collaboration], *Nucl. Phys. Proc. Suppl.* **196** (2009) 371 [arXiv:0902.0252 [astro-ph.IM]].
25. D. D. Dzhappuev, V. B. Petkov, A. U. Kudzhaev, N. F. Klimenko, A. S. Lidvansky and S. V. Troitsky, arXiv:1511.09397 [astro-ph.HE].
26. D. D. Dzhappuev, I. M. Dzaparova, E. A. Gorbacheva, I. S. Karpikov, M. M. Khadzhiev, N. F. Klimenko, A. U. Kudzhaev, A. N. Kurennya, A. S. Lidvansky and O. I. Mikhailova, *et al.* *EPJ Web Conf.* **207** (2019), 03004 [arXiv:1812.02663 [astro-ph.HE]].
27. See Supplemental Material at [URL to be inserted by publisher].
28. M. G. Aartsen *et al.* [IceCube], *Eur. Phys. J. C* **79** (2019) 234 [arXiv:1811.07979 [hep-ph]].

Supplemental material to
“*Carpet-2* search for gamma rays above 100 TeV in coincidence with
HAWC and IceCube alerts”

D. D. Dzhappuev et al. (Carpet-2 Group)

This Supplemental Material presents results of the search for $E > 100$ TeV photons associated with individual alerts. Table 2 gives the list of alerts, Tables 3 and 4 present the numbers of expected and observed (in 24-hour and 30-day time windows) photon-candidate events and upper limits on fluxes and fluences for $E > 100$ TeV and $E > 300$ TeV, respectively. Table 5 presents the same quantities for 1000-second time windows for two alerts whose arrival direction was in the Carpet-2 field of view at the event arrival time.

type	ID	MJD	RA, °	DEC, °
HAWC	H190806A	58701.556	78.4	6.6
HAWC	H190917A	58743.052	321.8	40.0
HAWC	H190927A	58753.954	248.7	21.2
HAWC	H191019A	58775.841	217.5	25.8
HAWC	H191208A	58825.557	228.9	40.2
HAWC	H200314A	58922.446	255.7	48.1
HAWC	H200814A	59075.901	177.8	19.9
HAWC	H200815A	59076.264	11.2	11.5
HAWC	H201019A	59141.905	203.1	29.7
HESE	I190331A	58573.289	355.6	71.1
EHE	I190503A	58606.724	120.3	6.4
GOLD	I190619A	58653.552	343.3	10.7
GOLD	I190730A	58694.869	225.8	10.5
GOLD	I191001A	58757.840	314.1	12.9
GOLD	I200109A	58857.987	164.5	11.9
GOLD	I200530A	58999.330	254.4	27.5
BRONZE	I190704A	58668.784	161.8	27.1
BRONZE	I190712A	58676.052	76.5	13.1
BRONZE	I191215A	58832.465	285.9	58.9
BRONZE	I191231A	58848.458	46.4	20.4
BRONZE	I200117A	58865.464	116.2	29.1
BRONZE	I200410A	58949.972	241.3	11.6
BRONZE	I200425A	58964.977	100.1	53.6
BRONZE	I200512A	58981.314	295.2	15.8
BRONZE	I200614A	59014.529	33.8	31.6
BRONZE	I200620A	59020.127	162.1	11.9
BRONZE	I200911A	59103.597	51.1	38.1
BRONZE	I200916A	59108.861	109.8	14.4
BRONZE	I200921A	59113.797	195.3	26.2
BRONZE	I201014A	59136.093	221.2	14.4
BRONZE	I201021A	59143.276	260.8	14.6

Table 2: List of alerts used in the present analysis. HAWC alerts are published at https://gcn.gsfc.nasa.gov/amon_hawc_events.html, HESE IceCube alerts were published at https://gcn.gsfc.nasa.gov/amon_hese_events.html, EHE IceCube alerts were published at https://gcn.gsfc.nasa.gov/amon_ehe_events.html, GOLD and BRONZE IceCube alerts are published at https://gcn.gsfc.nasa.gov/amon_icecube_gold_bronze_events.html. We add “H” for HAWC or “I” for IceCube to the official alert ID for clarity. MJD gives the event time as a Modified Julian Day, R.A. and DEC are equatorial coordinates in degrees.

E > 100 TeV limits

ID	24 hours			30 days			
	n_{expected}	$F_{95},$	$\mathcal{F}_{95},$	n_{observed}	n_{expected}	$F_{95},$	$\mathcal{F}_{95},$
		$10^{-11}\text{cm}^{-2}\text{s}^{-1}$	GeV/cm^2			$10^{-11}\text{cm}^{-2}\text{s}^{-1}$	GeV/cm^2
H190806A	0.0009	1790.	154.	0	0.0262	59.	153.
H190917A	0.0170	49.9	4.31	1	0.5093	2.37	6.13
H190927A	0.0060	172.	14.9	2	0.1809	11.7	30.4
H191019A	0.0092	109.	9.44	0	0.2747	3.32	8.6
H191208A	0.0167	49.7	4.3	0	0.5013	1.39	3.6
H200314A	0.0179	47.9	4.14	0	0.5360	1.32	3.42
H200814A	0.0052	199.	17.2	0	0.1556	6.31	16.4
H200815A	0.0021	650.	56.2	0	0.0636	21.2	55.
H201019A	0.0113	80.4	6.95	1	0.3396	3.96	10.3
HAWC stacked	0.0862	10.2	0.88	4	2.5871	0.77	1.99
I190331A	0.0054	201.	17.4	0	0.1618	6.35	16.5
I190503A	0.0007	1890.	163.	0	0.0222	62.4	162.
I190619A	0.0019	747.	64.6	1	0.0582	39.	101.
I190730A	0.0017	774.	66.9	0	0.0516	25.4	65.8
I191001A	0.0024	517.	44.7	0	0.0720	16.8	43.7
I200109A	0.0021	609.	52.6	1	0.0618	31.7	82.3
I200530A	0.0106	94.8	8.19	0	0.3182	2.83	7.34
I190704A	0.0104	97.9	8.46	0	0.3111	2.93	7.61
I190712A	0.0024	501.	43.3	0	0.0733	16.3	42.3
I191215A	0.0134	70.8	6.12	0	0.4013	2.05	5.32
I191231A	0.0057	188.	16.2	1	0.1702	9.59	24.8
I200117A	0.0109	83.9	7.25	2	0.3262	5.59	14.5
I200410A	0.0019	639.	55.2	0	0.0556	20.9	54.2
I200425A	0.0167	54.9	4.74	0	0.5018	1.53	3.97
I200512A	0.0037	336.	29.	0	0.1116	10.8	28.
I200614A	0.0136	71.	6.14	0	0.4080	2.05	5.32
I200620A	0.0022	609.	52.6	0	0.0667	19.9	51.5
I200911A	0.0168	52.6	4.54	3	0.5027	4.27	11.1
I200916A	0.0029	410.	35.5	0	0.0862	13.3	34.5
I200921A	0.0100	106.	9.12	0	0.2996	3.18	8.23
I201014A	0.0029	410.	35.5	0	0.0880	13.3	34.5
I201021A	0.0034	399.	34.4	0	0.1022	12.8	33.3
IceCube stacked	0.1417	6.82	0.59	8	4.2502	0.81	2.10

Table 3: Results of the search of $E > 100$ TeV photons. Alert IDs are defined in Table 2. For a given time period, 24 hours or 30 days centered at the alert, n_{expected} and n_{observed} are the expected and observed numbers of photon-like events from the alert direction, respectively ($n_{\text{observed}} = 0$ for all cases for 24 hours); F_{95} and \mathcal{F}_{95} are the 95% CL upper limits on the flux and fluence of the putative burst associate with the alert.

$E > 300$ TeV limits

ID	24 hours			30 days			
	n_{expected}	$F_{95},$ $10^{-11}\text{cm}^{-2}\text{s}^{-1}$	$\mathcal{F}_{95},$ GeV/cm^2	n_{observed}	n_{expected}	$F_{95},$ $10^{-11}\text{cm}^{-2}\text{s}^{-1}$	$\mathcal{F}_{95},$ GeV/cm^2
H190806A	0.0006	1350.	351.	0	0.0182	44.9	349.
H190917A	0.0102	38.	9.84	1	0.3053	1.88	14.6
H190927A	0.0033	131.	33.9	2	0.0982	9.02	70.1
H191019A	0.0049	83.	21.5	0	0.1480	2.64	20.5
H191208A	0.0102	37.8	9.8	0	0.3058	1.14	8.83
H200314A	0.0119	36.4	9.44	0	0.3564	1.07	8.35
H200814A	0.0031	151.	39.2	0	0.0929	4.89	38.
H200815A	0.0014	493.	128.	0	0.0427	16.2	126.
H201019A	0.0065	61.1	15.8	0	0.1964	1.91	14.8
HAWC stacked	0.0521	7.84	2.03	3	1.5640	0.55	4.27
I190331A	0.0030	153.	39.5	0	0.0889	4.94	38.4
I190503A	0.0005	1430.	371.	0	0.0160	47.5	369.
I190619A	0.0014	567.	147.	1	0.0413	29.7	231.
I190730A	0.0010	588.	152.	0	0.0311	19.4	151.
I191001A	0.0015	393.	102.	0	0.0440	12.9	100.
I200109A	0.0014	462.	120.	0	0.0427	15.2	118.
I200530A	0.0055	72.	18.7	0	0.1640	2.27	17.7
I190704A	0.0054	74.4	19.3	0	0.1631	2.35	18.3
I190712A	0.0013	380.	98.6	0	0.0387	12.5	97.4
I191215A	0.0083	53.8	14.	0	0.2480	1.65	12.8
I191231A	0.0034	143.	37.	1	0.1009	7.38	57.4
I200117A	0.0059	63.8	16.5	0	0.1778	2.	15.6
I200410A	0.0012	485.	126.	0	0.0347	16.	124.
I200425A	0.0104	41.7	10.8	0	0.3111	1.25	9.73
I200512A	0.0019	255.	66.2	0	0.0582	8.35	64.9
I200614A	0.0070	54.	14.	0	0.2111	1.68	13.
I200620A	0.0012	462.	120.	0	0.0364	15.2	118.
I200911A	0.0095	40.	10.4	1	0.2836	1.99	15.5
I200916A	0.0019	312.	80.8	0	0.0564	10.2	79.3
I200921A	0.0054	80.2	20.8	0	0.1609	2.53	19.7
I201014A	0.0016	312.	80.8	0	0.0476	10.2	79.5
I201021A	0.0020	303.	78.4	0	0.0587	9.89	76.9
IceCube stacked	0.0805	5.28	1.37	3	2.4151	0.32	2.51

Table 4: Results of the search of $E > 300$ TeV photons. See Table 3 for notations.

1000-second limits				
ID	$E > 100 \text{ TeV}$		$E > 300 \text{ TeV}$	
	$F_{95},$	$\mathcal{F}_{95},$	$F_{95},$	$\mathcal{F}_{95},$
	$10^{-11} \text{cm}^{-2} \text{s}^{-1}$	GeV/cm^2	$10^{-11} \text{cm}^{-2} \text{s}^{-1}$	GeV/cm^2
I190331A	7124.	7.12	5405.	16.2
I191215A	1065.	1.07	808.	2.43

Table 5: Results for alerts in the field of view (1000 s time window). See Table 3 for notations.